Influence of Horizontal Distance Between Earthmoving Vehicle Load and Deep Excavation on Support Structure Response

Ping Zhao [1], Zhanqi Wang [2], Youqiang Qiu [3] and Panpan Guo [4],*

1 School of Architecture and Engineering, Tongling University, Tongling 244000, China; 298839@tlu.edu.cn
2 School of Mining Engineering, Anhui University of Science and Technology, Huainan 232001, China; wangzq2023@aust.edu.cn
3 CCCC First Highway Consultants Co., Ltd., Xi'an 710075, China; b20200022@xs.ustb.edu.cn
4 School of Civil Engineering, Hefei University of Technology, Hefei 230009, China
* Correspondence: pp_guo@zju.edu.cn

Abstract: The objective of this paper is to investigate the influence of earthmoving vehicle load position on the deformation and internal force characteristics of a deep excavation (DE) support structure. The position of the earthmoving vehicle load near a DE is described by the horizontal distance between the earthmoving vehicle load and the DE. A two-dimensional finite element model is established for simulating DE engineering under the earthmoving vehicle load. The load of the earthmoving vehicle is treated as the static load, and the influence of the earthmoving vehicle load on the excavation support structure is considered from the static point of view. The numerical results of the finite element model agree well with the measured data from the field, which verifies the validity of the model. On the basis of this model, multiple models are established by changing the horizontal distance (*D*) between the earthmoving vehicle and the DE. The influence of *D* on the support structure and its critical magnitude for ensuring safety were studied. The results show that the underground diaphragm wall (UDW) is the main component for which horizontal displacement occurs under the earthmoving vehicle load. The horizontal displacements of the support structure exhibit an asymmetric distribution. When *D* decreases from 20 m to 0.5 m, the horizontal displacement of the UDW near the loading side increases, and the maximum horizontal displacement occurs at the top of the excavation support structure. The critical magnitude of *D* for ensuring safety is found to be 1 m. When *D* is less than 1 m, the DE is in an unsafe state. The UDW is the main component subject to the bending component. The bending moment distribution exhibits an "S" shape. The maximum bending moment increases with the decrease in *D*, and it occurs at the intersection of the second support and the UDW. As *D* decreases, the axial force in the first internal support changes from pressure to tension. The axial forces in the second and third internal supports are both pressures. The axial force in the third internal support is the largest. The research results have a positive effect on the design and optimization of DE support structures under the earthmoving vehicle load.

Keywords: earthmoving vehicle load; deep excavation; excavation support structure; stress field analysis; static deformation

1. Introduction

In recent years, China's population has continued to gather in large and medium-sized cities, which puts forward new requirements for the urban carrying capacity [1–5]. Due to the limited available land in the city, making full use of urban underground facilities has become a hot topic in urbanization development in recent years. DE engineering plays an important role in the construction of city infrastructure. As a significant means of city development and underground facility development, DE engineering presents two new characteristics at this stage. First, the excavation area and depth of the DE have increased significantly. The scale and complexity of DE engineering have undergone tremendous

growth. Second, due to the strict restrictions of the surrounding environment in dense urban areas, DE engineering is often faced with complex and sensitive boundary conditions and load conditions [6–9]. In addition, DE will produce a lot of earth and rock. Due to the effects of various factors such as self-weight and rainfall, the long-term accumulation of earth and rock near the DE will have a negative influence on the safety and stability of the DE [10–13]. Therefore, for the security of the DE, the earth and rock usually need to be transported to a place far from the construction site as soon as possible by using reliable transportation equipment.

An earthmoving vehicle refers to a truck transporting earth and rock excavated at the construction site. As the earthmoving vehicle has the advantages of high strength and strong loading capacity, it not only improves the efficiency of transporting earth and rock but is also relatively safe and reliable. Therefore, it is widely used for transporting earth and rock in construction sites. On the other hand, because of the restrictions of site work conditions, it is important for construction personnel to set up temporary construction roads near the DE. Thus, it is more convenient for earthmoving vehicles with a large load capacity to pass through and facilitate earthmoving transportation. However, when the road construction is relatively close to the DE support structure, the load generated during the passing of heavy earthmoving vehicles will impose a large effect on the ground stress near the DE [14–16]. Then, it causes the displacement of the DE and even damage. The displacement behavior of the DE under the load of adjacent earthmoving vehicles may show different characteristics from that of a general DE. If the design scheme is proceeded on the basis of the conventional method, there may be safety hazards and even engineering accidents, resulting in significant personal and property losses [17–20].

Studies related to DE have been given more attention by scholars, and many advancements have been achieved [21–25]. In previous works, Guan et al. [26] analyzed the scheme of shield tunnel displacement induced by DE and precipitation. Zhu et al. [27] carried out many studies on the influence of structure and soil displacement caused by DE. Moreover, Liu et al. [28] introduced the classification of DE in some tunnels and summarized the prediction method of the affected area of DE. Li et al. [29] established a differential formula and derived the analytical solution of tunnel deformation and internal force. In addition, Li et al. [18,30–32] studied the security of a DE and compared the prediction information with the real information. Wang et al. [18] carried out a study on the support technology of a DE near a railway based on displacement guidance. Cheng et al. [33] studied the simplified calculation method of ground lateral displacement resulting from DE. An investigation by Yang et al. [34] indicated that the friction angle is a significant factor affecting the deformation of the DE. Ge et al. [35] analyzed the influence of DE on the support structure deformation.

To sum up, the effects of DE under various conditions have been given more attention by scholars. On one hand, the study methods can be mainly categorized into three kinds, which are the numerical simulation method, the field monitoring method and the theoretical calculation method. On the other hand, the research object is the DE engineering of a subway station. In addition, studies are usually carried out under symmetrical conditions. Meanwhile, the research content mainly includes the effects of DE on the horizontal displacement of surrounding soil and the vertical deformation of the DE bottom. However, in the current relevant studies, there are few results on the influence of the earthmoving vehicle and the DE horizontal distance on the excavation support structure and its safety critical value [14,36,37]. In addition, due to the shortage of urban land, the environment around the DE is often complicated. The position of the unfavorable effect generated by earthmoving vehicles may change near the DE, and the situation is complicated. Furthermore, the load of earthmoving vehicles running near the top will have an impact on the stratum, which is not conducive to the safety of the DE [38–40]. In addition, how calculating the overload caused by vehicle load on the DE has always been a difficult task regarding DE [41,42]. In the past, the influence of earthmoving vehicle load was seldom considered in the DE support. In addition, the guidance on the specifications of DE, whether to consider the

impact of vehicle loads around the DE in the design and how to consider such dynamic loads, is unclear. The result is insufficient in the design of DE support [43,44]. In addition, it is of great significance to optimize and analyze the stability of the deep excavation support structure to obtain a more stable support structure under load [45,46].

Therefore, it is important to conduct research on the effect of the horizontal distance between the earthmoving vehicle and the DE on the support structure and its safety critical value. In view of this, based on the pre-existing studies, this paper is aimed at investigating the influence of the horizontal distance between the earthmoving vehicle load and the deep excavation on the support structure response. The research content mainly includes three parts. Firstly, this paper describes the load characteristics of the earthmoving vehicle and carries out an equivalent treatment of the load generated by the earthmoving vehicle. Secondly, finite element analysis software is adopted to establish the models (the software used in this study is described in reference [47]). Thirdly, the deformation rule of the support structure induced by the construction under the pressure of an earthmoving truck is studied, and the simulation results of the model are compared with the measured results. Finally, the effects of the horizontal distance between the earthmoving vehicle and the DE on the support structure and its safety critical value are analyzed. The research conclusions provide a helpful reference for similar engineering projects and further theoretical research.

2. Characteristics of Earthmoving Vehicle Loads and Their Equivalents

An earthmoving vehicle load refers to the load acting on the road surface through the wheels of an earthmoving vehicle. Obviously, the load of the earthmoving vehicle is mobile. In addition, the earthmoving vehicle may move at an uneven speed and generate momentum. Therefore, the load distribution of earthmoving vehicles has the characteristics of non-centralized distribution. Considering the rationality of the vehicle load value, this paper conducted a field investigation on a project under construction in Hefei, collecting relevant information, and measured the actual weight of the earthmoving vehicle when it was fully loaded. The earthmoving vehicle model in this study is the new M3000 dump truck from Shaanxi Automobile Heavy Cardron (SX3310MB426), Name of manufacturer: Shaanxi Automobile Group Co., Ltd., Xi'an, China. The body is 10.8 m long, 2.5 m wide and 3.5 m high. In addition, Figure 1 depicts the earthwork wheel spacing. Obviously, the earthmoving wheel distance is 2.5 m. The wheelbases are 1.8 m, 3.6 m and 1.4 m, respectively. In addition, the earthmoving car has four rows of wheels. Rows 1 and 2 are the front axles, and rows 3 and 4 are the middle and rear axles. It should be noted that the weight of the empty earthmoving vehicle is 20 tons. After full earthmoving, the actual total weight of the earthmoving truck is 60 tons.
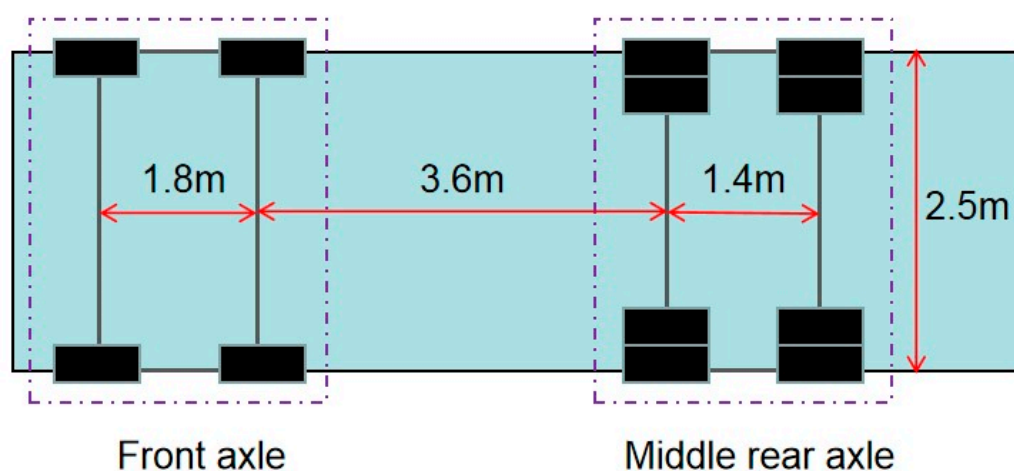

Figure 1. Diagram of wheel distance of earthmoving vehicle.

It should be noted that the main mechanical equipment of this foundation pit excavation is the Komatsu excavator (model: PC270-8), Komatsu Production Co., Ltd., Tokyo, Japan. The full load weight of this excavator is about 28 tons. Compared with the earthmoving vehicle (60 tons) filled with soil, the weight of the excavator is much lower. Moreover, the wheel of the excavator is a track, and the contact area between the wheel and the ground is much larger than that of the earthmoving vehicle. Therefore, relatively speaking, the excavator wheel exerts less force on the contact surface. In addition, the length of the foundation pit in this study is about 800 m, and the working face of the excavator is relatively small, which will not affect the entire foundation pit. In addition, the earthmoving vehicle will leave the excavator after loading the soil. It is worth noting that in the process of earthmoving vehicle transportation, there may be a mechanical failure of the fully loaded earthmoving vehicle, which cannot be driven at the side of the deep excavation. Also, the other loaded earthmoving trucks need to continue transporting earthmoving. In this case, there will be two fully loaded earthmoving vehicles near the foundation pit, which will cause more adverse effects. In view of this, the influence of the most unfavorable load on the excavation of the foundation pit is studied. This study did not consider the effect of the excavator and earthmoving vehicle together but considered the effect of two earthmoving vehicles loaded with soil near the foundation pit at the same time. This happens far away from where excavators operate. Therefore, in this study, the situation of two fully loaded earthmoving vehicles in parallel is regarded as the most unfavorable load arrangement. The vehicle spacing is 0.5 m. Figure 2 shows the diagram of the earth wheel spacing for the most unfavorable load arrangement.
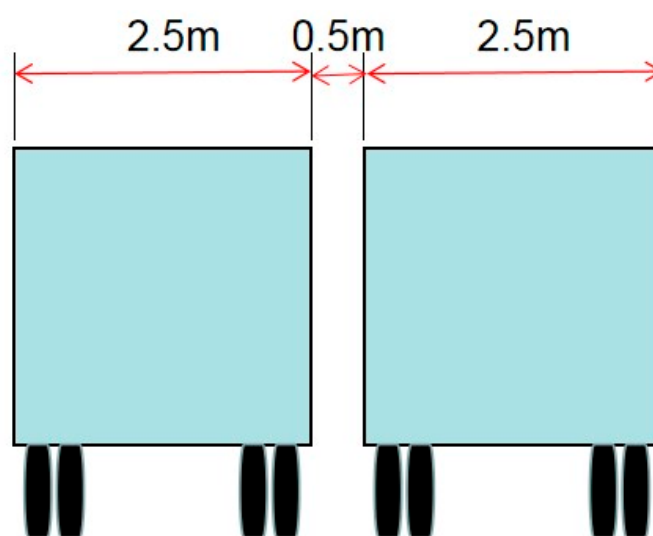
Figure 2. Position diagram of earthmoving vehicle under the most unfavorable load arrangement.

For the convenience of finite element analysis, it is essential to simplify the load of the earthmoving vehicle. In this study, the vehicle load is equivalent to the static load, and the influence of earthmoving vehicle load on the support structure is considered from the static point of view. The relevant research results show that the weight of the middle and rear axle of the earthmoving truck accounts for more than 80% of the weight of the vehicle [48–50]. In this study, the weight of the middle and rear axles is 80% of the total vehicle weight. It should be noted that, due to the emphasis on the study's central point, this research holds the gravity of the middle and rear axles of the loaded earthmoving vehicles to carry out a study on the effect of DE. In addition, the wheel has a certain contact area with the road surface, and the wheels on both sides of the same axle also have a certain distance. Also, there is a certain distance between the middle and rear axles. To improve research efficiency, the range of action of the rear axle on the contact surface of the earthmoving truck is approximately regarded as a regular rectangle. In addition, one side

of the rectangle measures 2.5 m, which corresponds to the width of the earthmoving vehicle itself. The length of the other side is close to the distance between the rear axles of the earthmoving truck, and the value is 1.2 m. The force acting on the surface of contact by the rear axle of the earthmoving truck is simplified as the uniform load q. The layout diagram of the most unfavorable load is shown in Figure 3. Additionally, taking a fully loaded earthmoving vehicle as an example, the concreteness calculation procedure of uniform load q is as follows:

$$G = m \times g = 60 \times 1000 \times 10 = 600 \text{ kN,} \tag{1}$$

$$G1 = G \times p = 600 \times 80\% = 480 \text{ kN,} \tag{2}$$

$$S = L \times W = 1.2 \times 2.5 = 3 \text{ m}^2, \tag{3}$$

$$q = G1 \div S = 480 \div 3 = 160 \text{ kPa.} \tag{4}$$

where G represents the gravity of the earthmoving vehicle; g is the acceleration of gravity; G1 indicates the pressure produced by the rear axle in the earthmoving truck; *p* represents the ratio of the pressure generated by the rear axle to the weight of the earthmoving vehicle; S is the equivalent load area; L is the equivalent load length; W is the width of equivalent load; and q is the equivalent load.
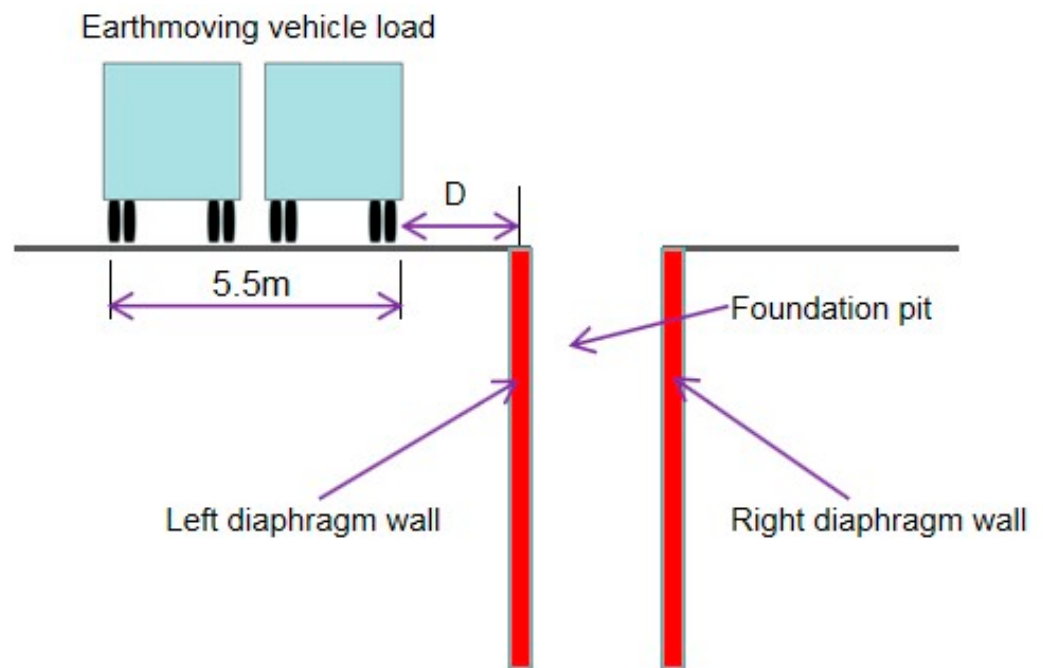

Figure 3. Schematic diagram of the most unfavorable load layout.

3. Project Overview

The object of this research is the DE engineering in a certain area of Hefei city. The excavation method of the foundation pit is open-cut. The section diagram of the DE is shown in Figure 4, where q is the load of the earthmoving vehicle, and *D* is the distance between the load and the DE. On the left of the DE, the soil produced by excavation is transported by earthmoving vehicles. It is a typical excavation project under the load of an earthmoving truck. The specific content of load characteristics and the equivalent of earthmoving vehicles are shown in the second part of this study. It should be noted that the space between the load of the earthmoving vehicle and the edge of the DE is *D* = 4 m. It has a range of 5.5 m. The equivalent uniform load is q = 160 kPa. In addition, the depth, length and width of the DE are 14 m, 836 m and 8 m, respectively, which is are typical in narrow strip DE [51]. In addition, the safety level of the side wall of the DE is level 1.
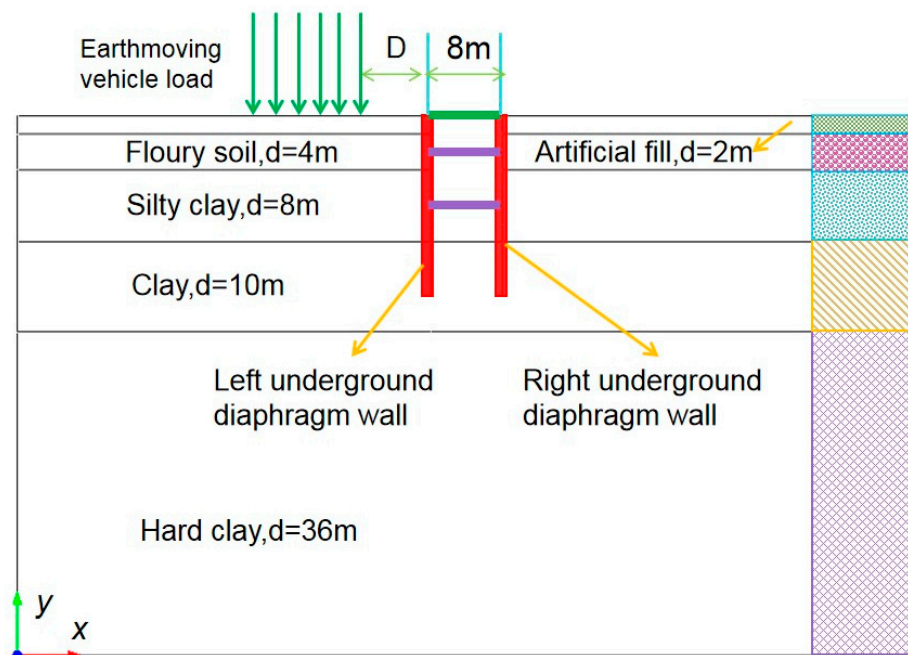
Figure 4. Section diagram of DE.

The retaining structure of DE is composed of UDW and three internal supports. The second and third internal supports are made of steel pipes. In addition, the top support is arranged 0 m below the surface. Moreover, the other two internal supports are arranged at 4 m and 10 m, respectively, below the ground surface. In addition, the UDW and the first support are made of concrete. Other relevant contents are shown in Table 1.

Table 1. Excavation support structure parameters.

Support Elements	Cross Section (mm)	Unit Weight (kN·m^3)	Elasticity Modulus, E (GPa)	Poisson's Ratio
Underground diaphragm wall	thickness = 500, total height = 20,000, embedment depth = 6000	24	20	0.2
First support	500 × 500, horizontal distance = 5000	24	20	0.2
Second support	diameter = 609, thickness = 12, horizontal distance = 5000	77	200	0.2
Third support	diameter = 609, thickness = 12, horizontal distance = 5000	77	200	0.2

The DE was performed in several steps. According to the geotechnical investigation report, the simplified soil layer has five layers. For details, see the schematic diagram of the DE section (Figure 4). The excavation depth is mainly silt and silty clay. Each excavation is carried out after the DE dewatering to 3 m below the construction face. The relevant information regarding the soil is shown in Table 2. The relevant meanings in Table 2 are consistent with reference [47].

Table 2. Mechanical parameters of soil layers.

| Soil Layer	E50ref (kN·m^{-2})	Eoedref (kN·m^{-2})	Eurref (kN·m^{-2})	v	γ (kN·m^{-3})	c (kN·m^{-2})	φ (°)	Thickness (m)
Artificial	4500	4500	13,500	0.2	20	10	12	2
Floury soil	7400	7400	22,200	0.25	18.1	14	15	4
Silty clay	9500	9500	28,500	0.32	18.5	18	16	8
Clay	10,700	10,700	32,100	0.35	18.9	22	16	10
Hard clay	13,500	13,500	40,500	0.25	18	30	20	36

4. Model Building and Numerical Calculation

4.1. Basic Assumptions

The construction process and site engineering conditions are complicated. There are several hypotheses in this study. One is that the earthmoving vehicle load is assumed to be uniformly distributed. This assumption is based on the content described in the section "2. Characteristics of earthmoving vehicle loads and their equivalents". The other one is that each layer of soil is distributed continuously and evenly [52,53]. Furthermore, other assumptions are consistent with reference [47].

4.2. Calculation Model

Finite element analysis software is used to establish a model for numerical simulation. The influence of the earthmoving truck load on the mechanical response of DE retaining structures is studied. Obviously, the DE is a narrow strip. Therefore, for non-pit corner regions, the plane strain can be used for analysis [54,55]. If the dimension of the model is small, the simulation results will be inaccurate. Conversely, the time of calculation will be prolonged. By changing the size of the model for trial calculation, the model width and height were determined (See Figure 5 for details). The model size is much larger than the predicted influence range of the DE. The meanings of x and y in Figure 5 are consistent with reference [47]. The model adopts standard boundary conditions. Only vertical displacement is allowed at the left and right borders. The top is a free boundary that allows horizontal and vertical movement. Moreover, the bottom cannot be moved. The displacement response of the soil around the DE has obvious small strain characteristics [17,18,56]. The soil constitutive model is consistent with reference [47]. In addition, the elastic constitutive relation is used for the envelope structure. The soil mass is a 2D plane element considering the plane strain. Furthermore, the UDW uses 1D beam units, as does the support.
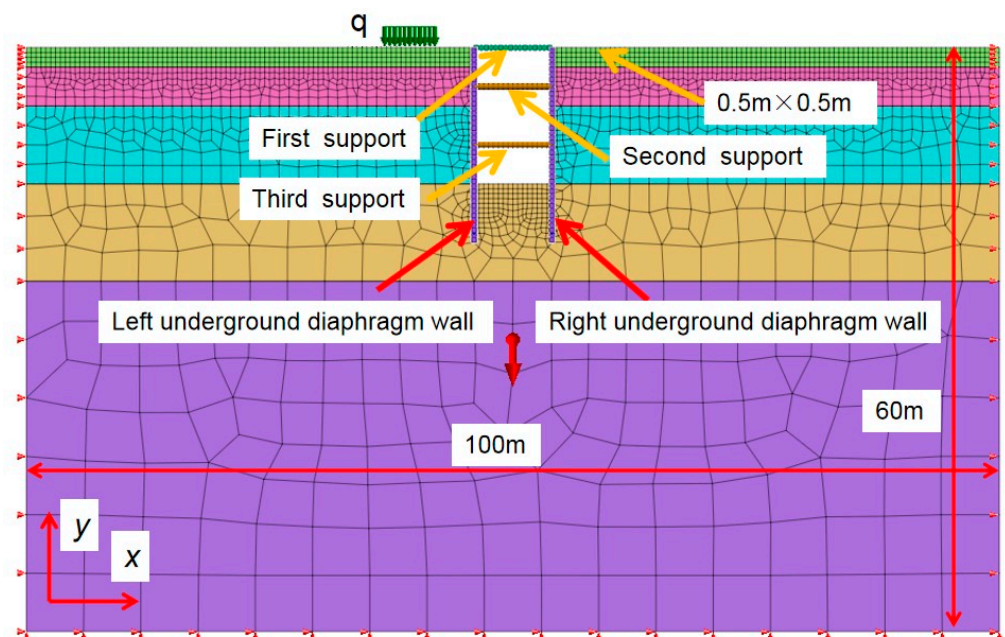
Figure 5. Numerical model.

4.3. Simulated Construction

To make the numerical simulation conform to the actual engineering situation, the related work of the DE is realized by finite element software. The process of DE mainly involves the installation of the UDW, soil excavation, and the setting of the internal support. In addition, the excavation simulation of the DE is controlled by the command "passivation" in the software. The setup's support is controlled by the command "Activate" in the

software. The specific construction process consists of nine parts, and the specific contents are shown in Table 3. It should be noted that the loading process in this study is performed one time: under working condition 2, the UDW is constructed. In addition, the earthmoving vehicle load is added, and the completion of DE in this study refers to working condition 9.

Table 3. Construction conditions.

Construction Conditions	Specific Contents
Construction condition 1	Initial geostress analysis, displacement clearing.
Construction condition 2	The UDW is constructed. In addition, the load of earthmoving vehicle is added.
Construction condition 3	Excavation 1: the DE is excavated 2 m below the surface and the first support is added.
Construction condition 4	Excavation 2: the DE is excavated 4 m below the surface.
Construction condition 5	Excavation 3: the DE is excavated 6 m below the surface, and the second support is installed.
Construction condition 6	Excavation 4: the DE is excavated to 8 m below the surface.
Construction condition 7	Excavation 5: the DE is excavated 10 m below the surface.
Construction condition 8	Excavation 6: the DE is excavated to 12 m below the surface, and add the third support.
Construction condition 9	Excavation 7: the DE is excavated 10 m below the surface.

## 5. Comparative of Simulation and Field Measurements

On-site monitoring can rapidly furnish the response to the real construction situation of the construction site. For example, by arranging monitoring points at the construction stage, monitoring instruments can be used to simultaneously obtain data such as the displacement and axial force of the UDW during the construction process. The construction parameters monitored on-site have relatively important reference values to verify the rationality of the calculation model. However, field monitoring is not predictive in advance. There are some limitations to the optimization and guidance of the project site. Furthermore, the numerical calculation model is relatively fast. The cost is relatively low. The calculation results are predictable. The disadvantage of the model is that the observed model may not accurately demonstrate the conditions of the project site. The two methods of monitoring and simulation are combined. Based on the premise of ensuring the model's rationality, the analysis is conducted, and the results exert a significant positive influence on effectively guaranteeing the safety and optimization of the deep excavation [24,34].

To demonstrate the reliability of the parameter values, the simulation information of the deformation of the UDW in condition 9 was extracted. It should be noted that according to the conclusions of other scholars [57,58], the load of earthmoving vehicles will generate a larger disadvantage influence on the structure near the load side. Due to the emphasis of the study's focus, the enclosure structure studied is the left UDW. The conclusions are contrasted with the monitoring values. The comparison chart is drawn. Figure 6 shows the comparison between the simulated deformation of UDW and the monitoring results under working condition 9.

Obviously, when the DE is completed, the field monitoring results demonstrate that the maximum displacement of the left UDW is about 14 mm. The maximum horizontal deformation occurs between the last support and the base of the DE. Evidently, the DE is in a safe state. This also reflects that the selection of the structure is reasonable. In addition, the excavation condition of DE is arranged properly. Furthermore, the simulation conclusions align well with the actual information. At the same time, it also reflects the reliability and rationality of the parameter values of the model. At the same time, it also shows that this study has a certain feasibility for evaluating the earthmoving vehicle load. In addition, the monitoring information is somewhat distinction from the numerical information, but the difference is small. This may be attributed to the fact the simulation cannot fully consider the complexity of the actual construction conditions, for example, the occurrence of rain at the construction site. The effect of rainfall was not taken into account when the model was built. The results of field monitoring are more robust than those of the numerical simulation, leading to a discrepancy between the simulation and the actual deformation. In summary, the displacement rules are similar. This demonstrates that the model of the

DE has a certain rationality. On this basis, the correlation analysis of the load and variant of the structure caused by the variation in *D* between the load of the earthmoving vehicle and the DE can be carried out.
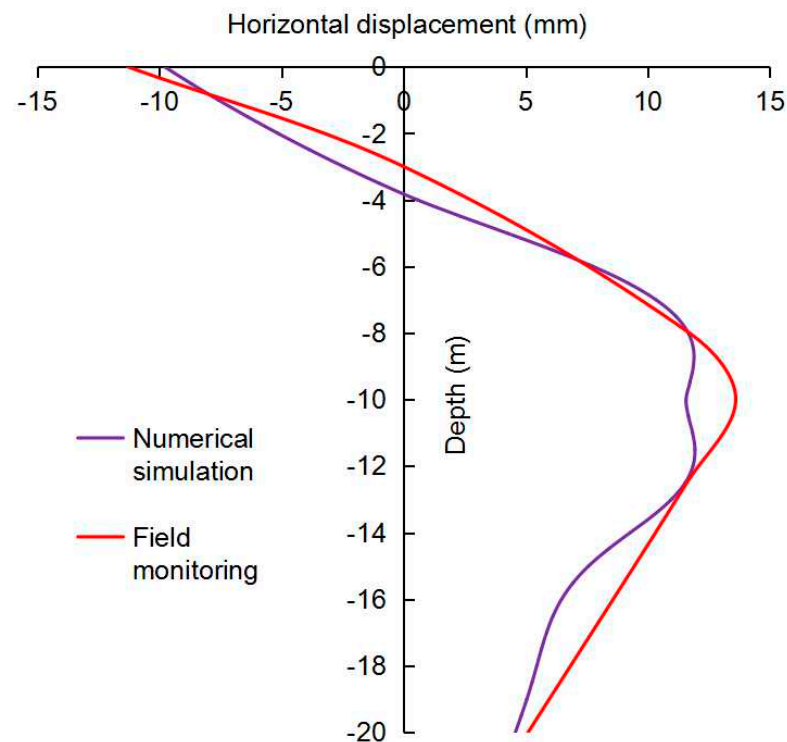

Figure 6. Comparison of simulated and monitored horizontal displacement of UDW.

6. Study on the Influence of the Horizontal Distance Between the Earthmoving Vehicle and the DE on the Support Structure and Its Safety Critical Value

In order to investigate the effect of changing the earthmoving vehicle load position on the deformation behavior of the DE support structure, the case where the load q is 160 kPa and the excavation depth equals 14 m is considered. In addition, the load width is 5.5 m. The calculation model was used to analyze the horizontal displacement and force changes in the DE support structures under the conditions of working condition 9, when the distance between the load of the earthmoving truck and the DE is *D* = 0.5 m, 1.0 m, 1.5 m, 2.0 m, 2.5 m, 4.0 m, 8.0 m, 16 m and 20 m. This research contains three parts: the displacement, the bending moment of the support structure and the axial force. The details are as follows.

6.1. Influence of Load Position of Earthmoving Vehicle on Displacement of Structure

The deformation of the support structure is a significant index to estimate the stability and safety of the enclosure structure of the DE [59,60]. Figure 7 reveals the displacement cloud map of the enclosure structure when the distance *D* between the load of the earthmoving vehicle and the DE is different. Obviously, the load of earthmoving vehicles will cause a deformation of the structure. The distance *D* between the load of the earthmoving truck and the DE is variable, and the deformation of the enclosure structure will change constantly. The nephogram of the structure presents asymmetric characteristics. This shows that the deformation on both sides of the structure is different. This demonstrates the deformation reaction of the structure is different under the load of earthmoving vehicles. Therefore, the reinforcement configuration of the UDW on both sides of the DE takes into account the actual situation affected by the load of earthmoving vehicles near the DE, specifically as the distance *D* decreases.
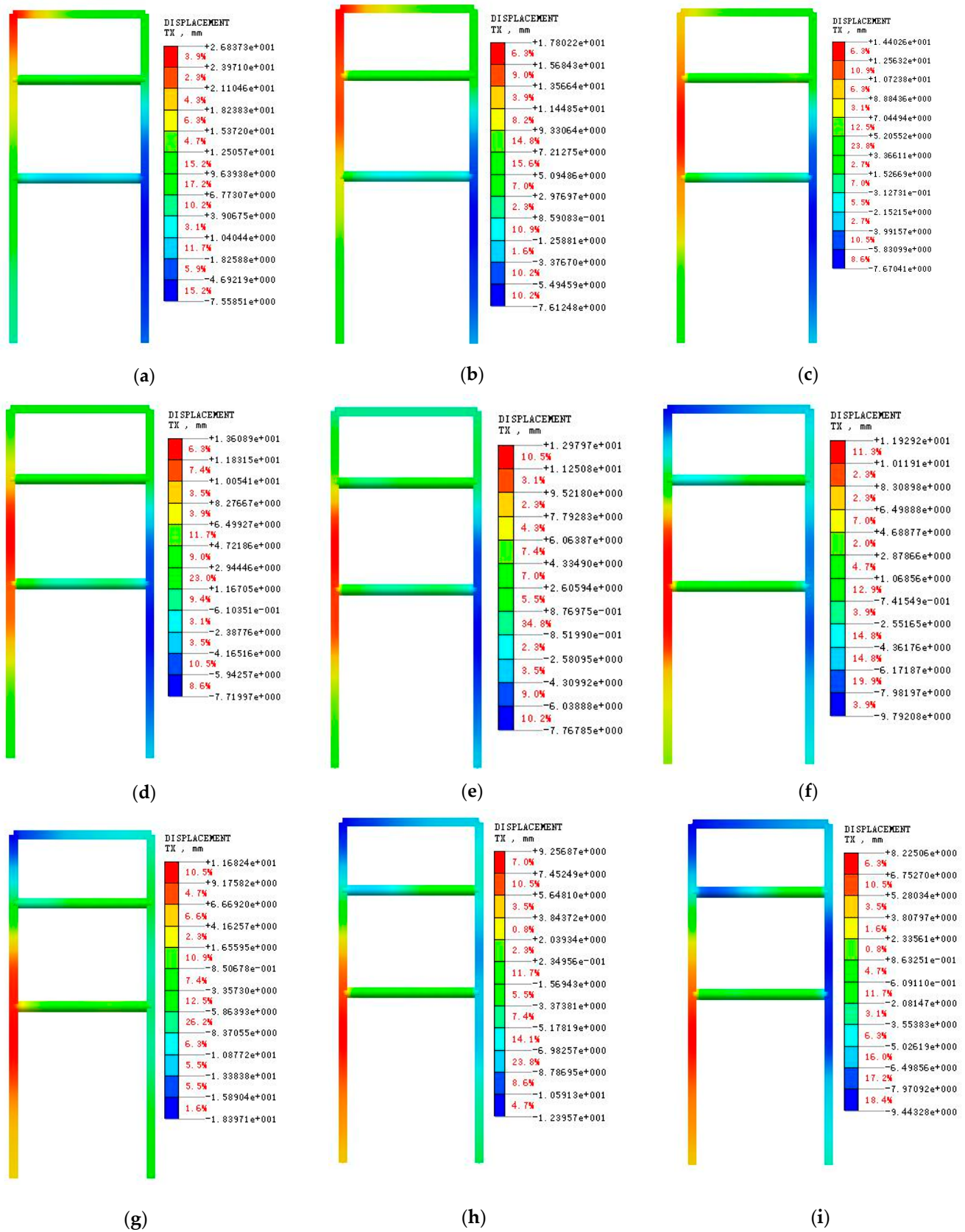
Figure 7. Horizontal displacement cloud image of enclosure structure when the position of the earthmoving vehicle load changes: (**a**) D = 0.5 m; (**b**) D = 1.0 m; (**c**) D = 1.5 m; (**d**) D = 2.0 m; (**e**) D = 2.5 m; (**f**) D = 4.0 m; (**g**) D = 8.0 m; (**h**) D = 16.0 m; (**i**) D = 20 m.

Overall, the deformation of the left structure presents an upward trend. The right side reveals a downward trend in general. It should be noted that when $D \leq 1$ m, the maximum values appear at the upper portion of the UDW. The value changes from 20 m to 1.5 m. As D becomes larger, the maximum displacement position gradually moves down. Therefore, it is crucial to consider the load position of earthmoving vehicles that may appear on the construction site when designing the support structure. In particular, we should pay attention to the checking calculation and on-site monitoring of the parts where the maximum displacement occurs to decrease the negative influence of the load of earthmoving vehicles on the DE.

In addition, the UDW is the main component where horizontal displacement occurs. It should be noted that although the support and the right UDW will also produce horizontal displacement under the load of earthmoving vehicles, the displacement is smaller when contrasted with the left UDW. To emphasize the study's focus, the effect of different distances D between the earthmoving truck load and the DE on the deformation of the left UDW is analyzed in detail.

In an attempt to achieve a better understanding of the effect of the D on the horizontal displacement of the UDW, the results from the numerical simulation are extracted. The column diagram of the maximum value of the left UDW is drawn, as shown in Figure 8. Obviously, as D continues to decrease, the maximum value of the UDW continues to increase. When $D = 20$ m, the maximum value is 8.2 mm. In addition, when $D = 0.5$ m, the value is 26.8 mm. The maximum value increased by about 227%. Furthermore, the maximum value of the UDW is greatly influenced by D. When the load of the earthmoving vehicle is closer to the DE, the value response is larger. Specifically, when D is gradually reduced from 20 m to 4 m, the maximum horizontal displacement increases from 8.2 mm to 11.9 mm. The maximum horizontal displacement increase is relatively small, no more than 3 mm. In addition, when D gradually decreases from 2.5 m to 1 m, the maximum horizontal displacement increases from 13 mm to 17.8 mm. The maximum horizontal displacement increase is relatively small and does not exceed 3 mm. It should be noted that when D ranges from 1 m to 0.5 m, the maximum horizontal displacement increases from 17.8 mm to 26.8 mm. The maximum horizontal displacement increase is 9 mm, which is nearly a 51 percent increase.
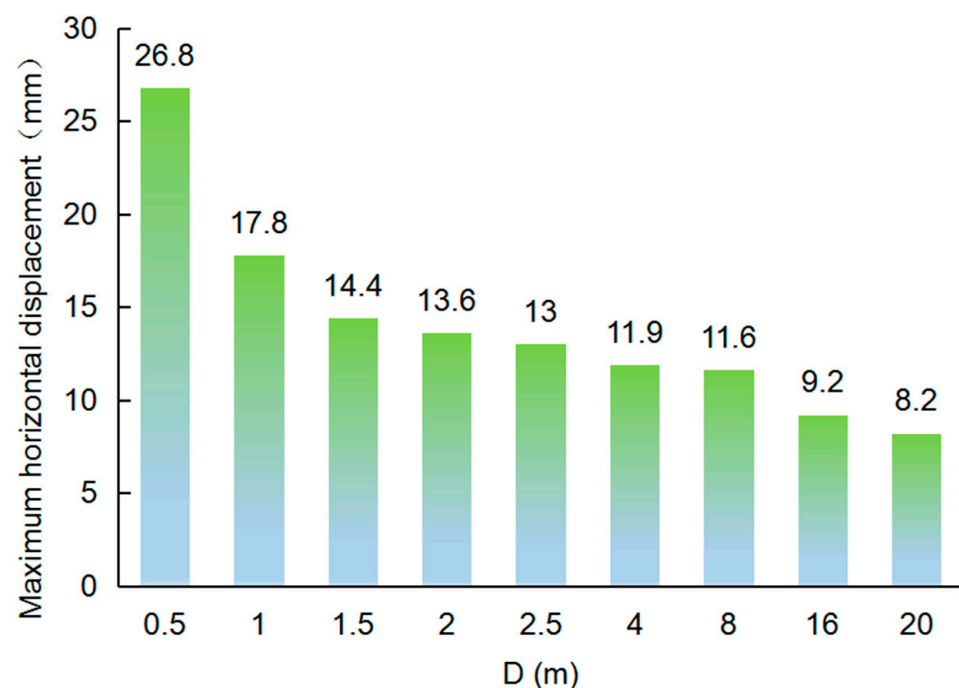

Figure 8. Comparison of maximum horizontal displacement of the left UDW.

In addition, through the implementation rules regarding DE and support in Hefei City, it can be found that the safety requirement of the UDW of the DE in this construction is level 1. The control value of the accumulated displacement of the enclosure structure by the DE monitoring is 0.0025 H (H is the depth of the DE), and is not greater than 30 mm. After calculation, the cumulative horizontal displacement control value of the excavation structure is 30 mm. In addition, the implementation rules stipulate that the pit deformation monitoring alarm value should be 70% to 80% of the monitoring control value. In this analysis, the monitoring alarm value of DE deformation is 70% of the monitoring control value. It is calculated that the monitoring and alarm value of DE deformation is 21 mm.

It should be noted that when $D = 0.5$ m, the maximum value is 26.8 mm, which exceeds the excavation deformation monitoring alarm value of 21 mm. At this time, the DE is in an unsafe state. When $D \geq 1$ m, the maximum value is smaller than the monitoring alarm value of the DE deformation, and the DE is in a secure state. Obviously, the D has a safety critical value, and the safety critical value is 1 m. When D is less than 1 m, the DE is in an unsafe state.

Therefore, if the site is limited, among other reasons, the earthmoving vehicle can be driven close to the DE. However, the safety threshold of D is 1 m. Therefore, it is necessary for the site management personnel to strengthen the management of the construction site. It is important to strictly control the D so that it is not less than 1 m.

The common law of the influence between the maximum value and the load position of an earthmoving vehicle is investigated. The calculated results of the maximum value of the UDW are fitted, and the fitting curve is formed. Figure 9 is a fitting graph. It should be noted that due to more intuitive research, the results calculated between the maximum value of the UDW, the variation in load position of the earthmoving vehicle and the maximum value of the left UDW are selected for drawing.
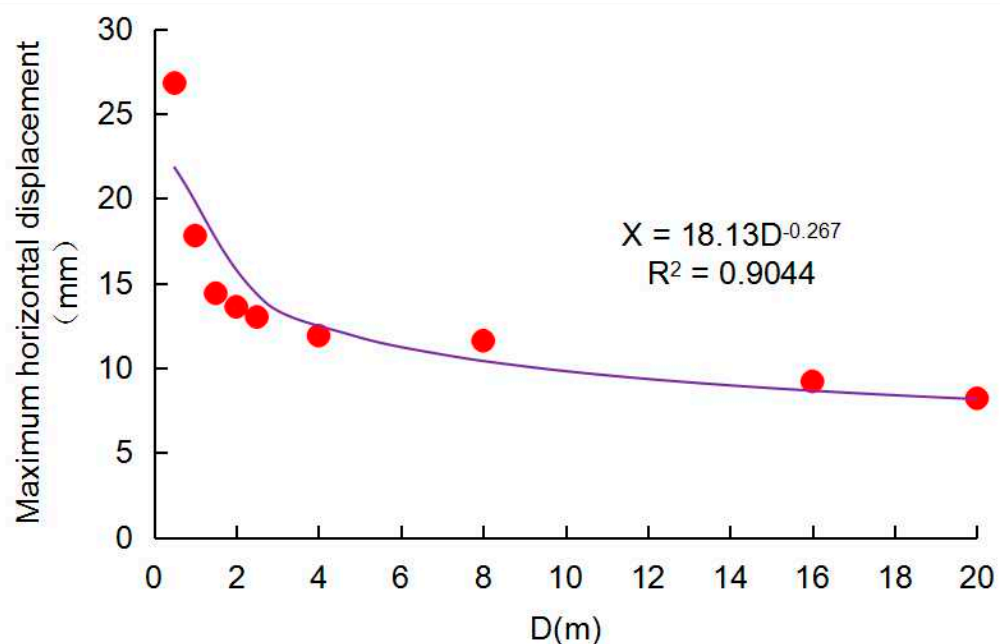
Figure 9. The relationship between maximum value and position of earthmoving vehicle shown by fitted curve.

Obviously, the maximum value X of the UDW varies with the change in the load position D of the earthmoving vehicle. When D decreases from 4 m to 0.5 m, the maximum value of UDW rises more and more, which will have an adverse effect on the DE. When D reduces from 20 m to 4 m, the maximum value of the UDW is enlarged too, but the increase is comparatively small. Therefore, project managers need to strictly manage the load of earthmoving vehicles that may appear near the DE. Meanwhile, strict control of the

distance D is important, ensuring that the DE is in a safe condition during excavation. In addition, there is a power function connection between the maximum value X and *D* of the UDW. Among them, the relationship between the maximum value of the UDW and the load position change in the earthmoving vehicle is exhibited in Formula (5). The calculated correlation coefficient (R^2) between X and *D* is 0.9044. The regression correlation coefficient R^2 is approximately 1. This means that the propinquity effect is reasonable.

$$X = 18.13 \times D^{-0.267} \tag{5}$$

6.2. Influence of Load Position of Earthmoving Vehicle on Bending Moment of Structure

The bending moment of the support structure system is a significant index for estimating the safety of the DE [36,61]. Figure 10 shows the cloud image of the bending moment when the loading position of the earthmoving vehicle is different. Obviously, the bending moment of the UDW and the support will be generated by the effect of the earthmoving vehicle. The diagram shows an "S" shape. The value varies with the load position of the earthmoving vehicle. Under the same conditions, the diaphragm wall is larger. The cloud image of the support structure presents asymmetrical graphic features.

It should be noted that the position of the maximum value of the UDW is different from the variations in the load position *D* of the earthmoving vehicle. Specifically, on one hand, when *D* < 4 m, it appears at the intersection of the second support and the UDW. On the other hand, when *D* ≥ 4 m, it appears at the junction of the third support and the UDW. In addition, the UDW is the main bending component. Despite the support also generating bending moment internal force, the value produced by the support is smaller when contrasted with the UDW. To emphasize the study focus, a detailed study on the impact of series load positions of earthmoving vehicles on the bending moment of the UDW is conducted.

The effect of *D* on the bending moment of the UDW is investigated. A comparison of the bending moment of the left UDW for various positions of the earthmoving vehicle load is shown in Figure 11. Obviously, the maximum value of the UDW enlarges with the decrease in *D*. Specifically, when *D* = 20 m, the maximum value is 123.9 kN·m. In addition, when *D* = 0.5 m, the maximum value is 193.6 kN·m. The maximum value is increased by about 56%. In addition, when *D* = 16 m, the maximum value is 128.9 kN·m. In addition, when *D* = 8 m, the maximum value is 150.6 kN·m. The maximum value is increased by about 17%.

Moreover, when the applied force of the earthmoving vehicle is closer to the DE, the bending moment response caused by it is larger, which needs to be paid great attention. In the process of DE, the greater the value generated by the enclosure structure under external action, the higher the required flexural stiffness of the structure. On the other hand, the construction site management personnel need to reinforce the management of the engineering. Strict control of the position between the vehicle and the DE is important to ensure the safety of the DE. In addition, it is important to reinforce the monitoring and protection of the bending moment and force of the UDW neighboring the load side of the earthmoving vehicle during load movement.

To further exhibit the common rule of the influence between the bending moment and the load position of the earthmoving vehicle, extract the numerical calculation results. The consequences of the maximum value of the UDW are fitted and the fitting curve is formed. Figure 12 shows the curve of the influence between the maximum bending moment of the UDW and the variation in the load position of the earthmoving vehicle. Obviously, the maximum value of the UDW varies with the variation in the load position of the earthmoving vehicle. When *D* decreases from 8 m to 0.5 m, the maximum value of the UDW increases more. The relationship curve is relatively steep and close to linear, which will have adverse effects on the DE. When D decreases from 20 to 8 m, the magnitude of the maximum bending moment of the UDW increases in a gentle manner. The increase is small.
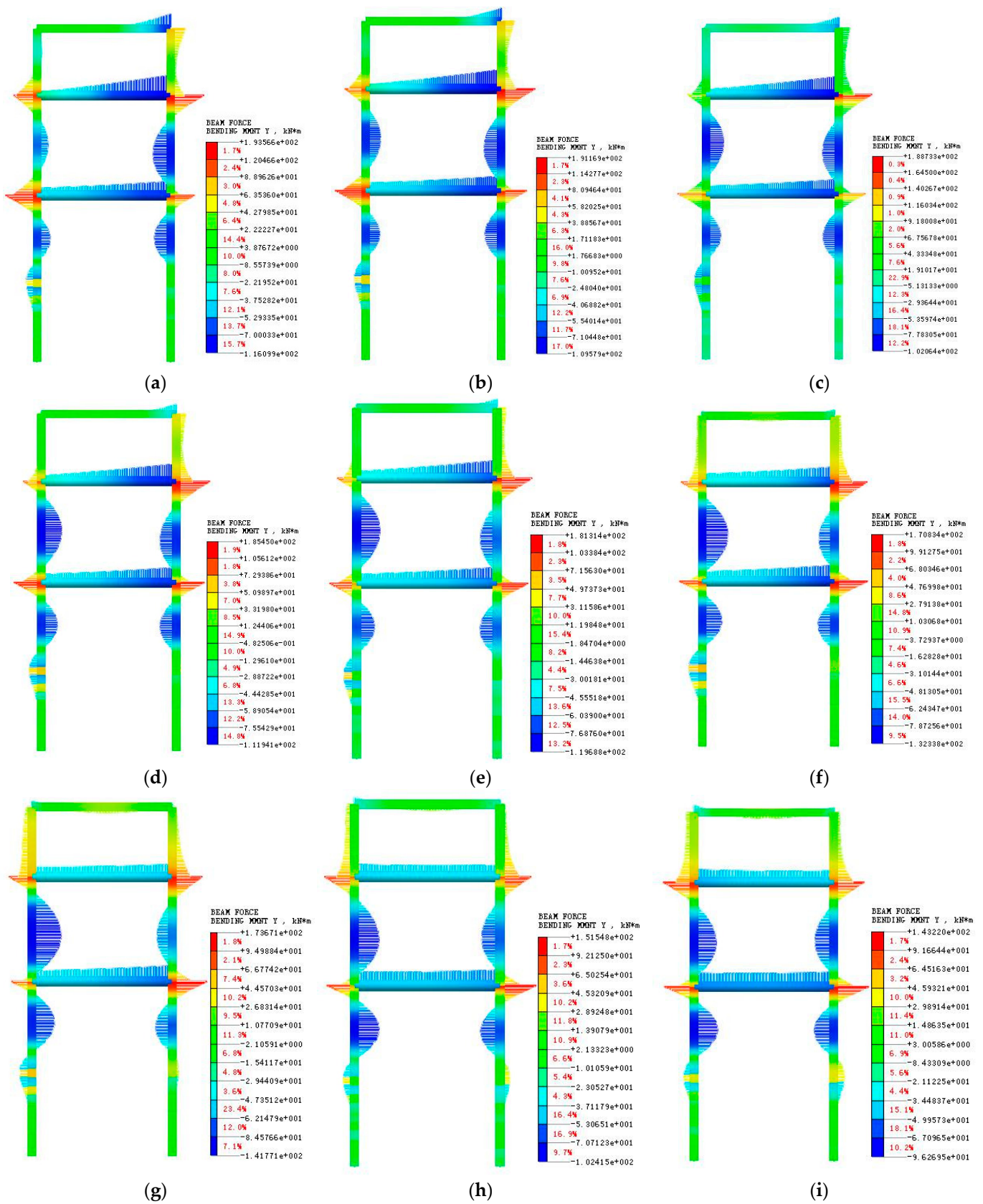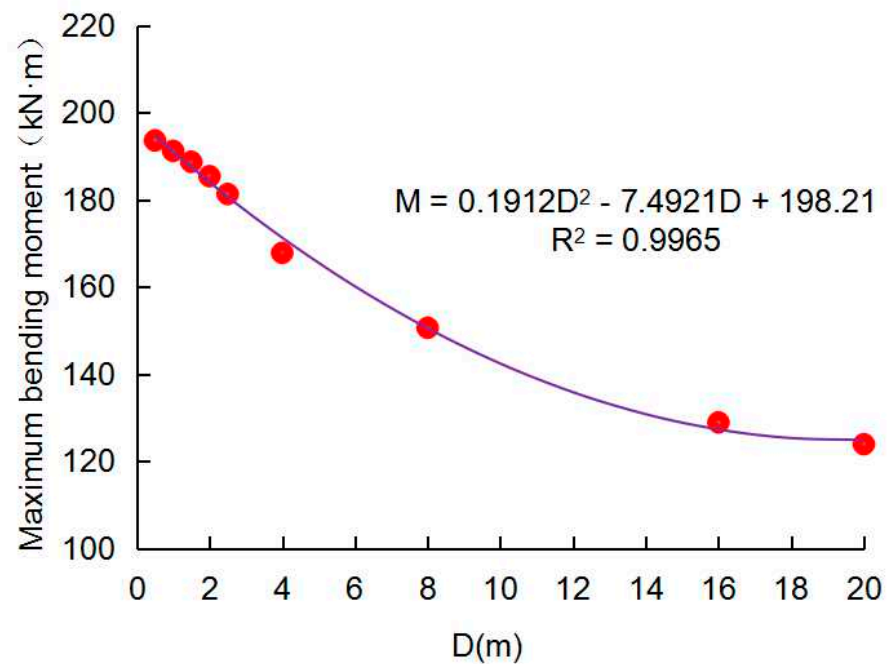
Figure 10. Bending moment cloud image of enclosure structure when the position of the earthmoving vehicle load changes: (**a**) D = 0.5 m; (**b**) D = 1.0 m; (**c**) D = 1.5 m; (**d**) D = 2.0 m; (**e**) D = 2.5 m; (**f**) D = 4.0 m; (**g**) D = 8.0 m; (**h**) D = 16.0 m; (**i**) D = 20 m.
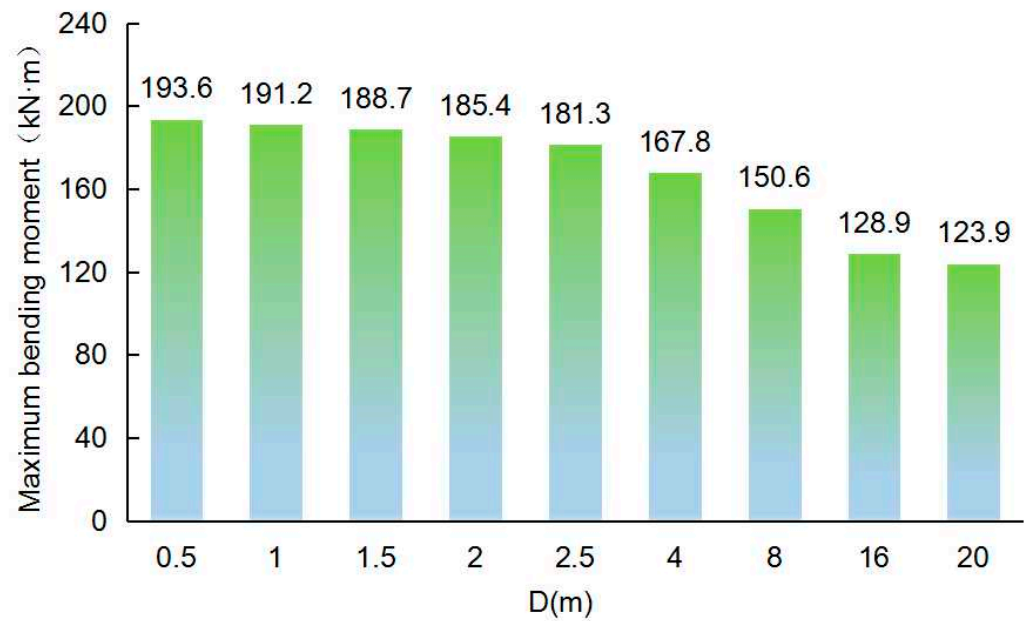
Figure 11. Comparison of bending moment of the left UDW when the position of the earthmoving vehicle load changes.


Figure 12. Fitting curve of the connection between the maximum bending moment of the left UDW and the position of the earthmoving vehicle load.

In addition, the connection between the maximum bending moment M and *D* of the diaphragm wall is a quadratic polynomial. Among them, the connection between the value of the UDW and the load position of the earthmoving vehicle is shown in Formula (6). The R^2 between M and *D* is 0.9965. The regression correlation coefficient R^2 is approximately 1. This means that the propinquity effect is reasonable.

$$M = 0.1912 \, D^2 - 7.4921 \, D + 198.21, \tag{6}$$

6.3. Influence of Load Position of Earthmoving Vehicle on Internal Supporting Axial Force

The axial force of the DE retaining structure will be generated under external load. Also, the support is the major component that generates axial force [62–66]. Due to the study focus, this research only selects the axial force achievements of the internal support for targeted research. Figure 13 shows the axial force cloud image when the load position of the earthmoving vehicle is different. Obviously, the load action of the earthmoving vehicle will cause the axial force of the support. In addition, the force of internal support is different at different positions. The axial force varies with the load position of the earthmoving vehicle. In addition, the values of different sections of the same internal support are the same. The support axis tries to form a "rectangle".
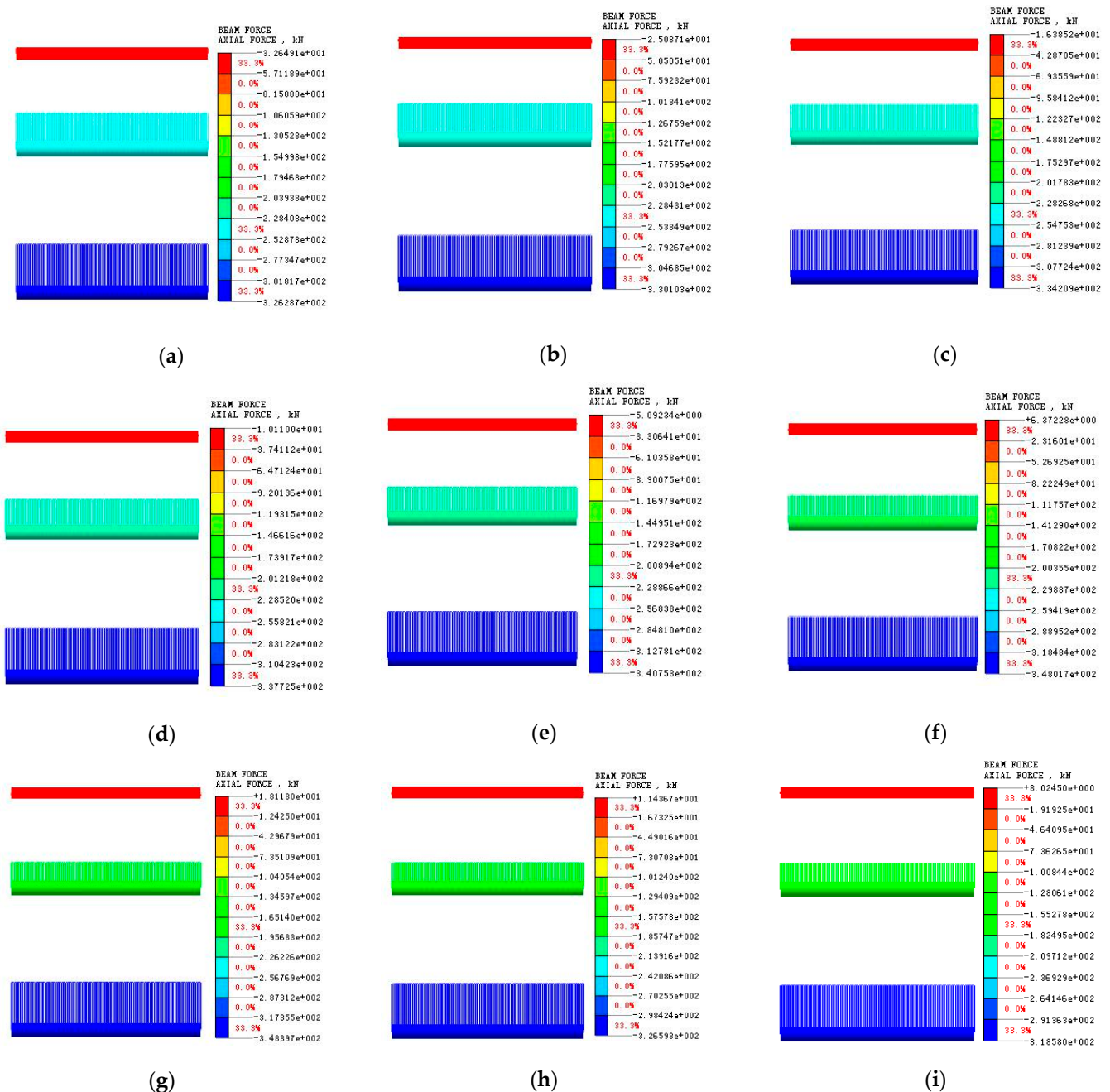
Figure 13. Axial force cloud image of support when load position of earthmoving vehicle is different: (**a**) D = 0.5 m; (**b**) D = 1.0 m; (**c**) D = 1.5 m; (**d**) D = 2.0 m; (**e**) D = 2.5 m; (**f**) D = 4.0 m; (**g**) D = 8.0 m; (**h**) D = 16 m; (**i**) D = 20 m.

It should be noted that when $D \leq 2.5$ m, the axial force is negative. The axial force of the first support is pressure. When $D \geq 4$ m, the axial force is tensile force. The main reasons are as follows ($D = 1$ m and $D = 20$ m are taken as examples for explanation): It is not difficult to find from the cloud image of the support structure in Figure 7 that when $D = 1$ m is completed, the upper of the left UDW has a displacement to the right of 17.8 mm. The top of the right diaphragm wall has a displacement of 2.9 mm to the left. The first support, attached to the upper of the UDW, is compressed and therefore subjected to axial force. In addition, when $D = 20$ m, when the excavation is completed, the top of the left UDW has a displacement of 9.4 mm to the left. The upper of the right side has a displacement of 5 mm to the left. Obviously, although the two sides have the same displacement, the left side is larger. The reason may be the first support, which is attached to the upper of the UDW and is stretched so that the axial force is pulled.

It should be noted that the results in Figure 13 are consistent with those of the structure in Figure 7 when the load position of the earthwork is different. The rationality and reliability of the model established in this study are verified again. In addition, we can also find that the forces of the second and third supports are pressure. Next, the results from the detailed study on the effect of changing the earthmoving vehicle position on the internal support axial force are discussed.

In order to investigate the effect of D on the internal support structure axial force, the results of the calculation are extracted as shown in Figure 14. In Figure 14, obviously, the force of the support constantly changes with D. The changing rules of the support in the three channels are variable. Due to the study focus and to analyze more intuitively, the force variation in the three supports is analyzed.
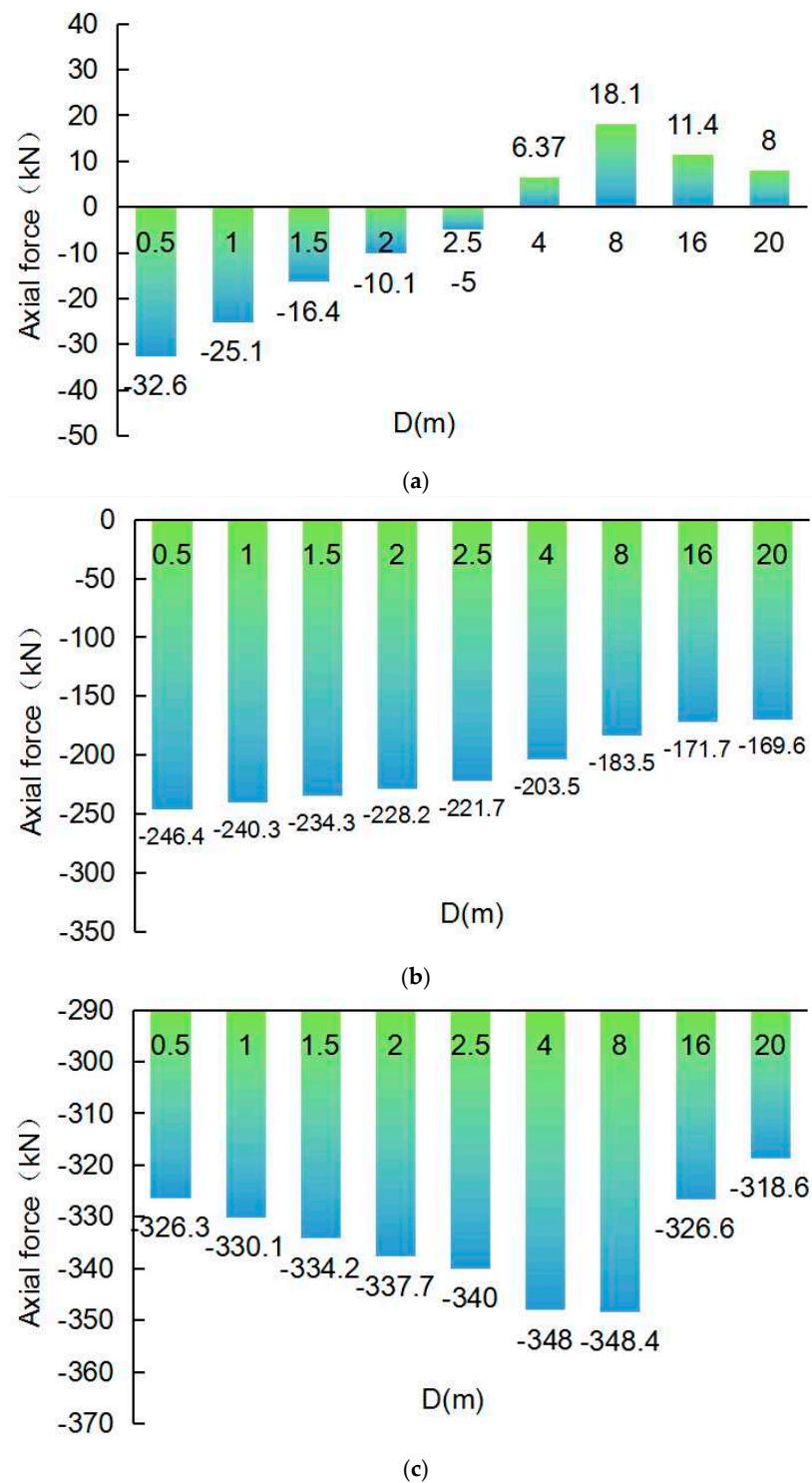
Figure 14a shows the axial force column diagram of the first support. Obviously, when decreases from 20 m to 0.5 m, the value of the top support exhibits a trend of "first increasing, then decreasing, and then increasing". Specifically, when $D = 20$ m, the value is +8 kN; obviously, the internal support is strained. In addition, when $D = 8$ m, the value is +18.1 kN; obviously, the internal support is strained too. The axial force value is increased by about 150%. Moreover, when $D = 2.5$ m, the value is −5 kN; obviously, the internal support is compressed. When $D = 0.5$ m, the maximum value is −32.6 kN; obviously, the internal support is compressed too. The axial force value increased by about 552%. Therefore, in the design of the first internal support, both the compression situation and the tension situation should be considered.

Figure 14b shows the axial force column diagram of the second support. Obviously, when D decreases from 20 m to 0.5 m, the value in the second support shows a trend of "increasing". Specifically, when $D = 20$ m, the axial force is −169.6 kN. When $D = 0.5$ m, the maximum axial force appears, which is −246.4 kN. The axial force value is increased by about 45%.

Figure 14c presents the axial force column picture of the third support. Obviously, when D decreases from 20 m to 0.5 m, the supporting axial force in the third channel presents a trend of "first increase, then decrease". Specifically, when $D = 20$ m, the axial force is −318.6 kN. When $D = 8$ m, the maximum value is −348.4 kN. The axial force value increased by about 9.4%. When $D = 0.5$ m, the axial force is −326.3 kN. The axial force value is reduced by about 6.3%. The second and the third support are both under pressure.

Therefore, in the design stage, it is necessary to focus on a compressive design and select materials with good compressive strength to make the second and third internal supports. In addition, by comparing Figure 14, it is not difficult to find that when D is the same, the relation between the value of the support is as follows: the third support > the second support > the first support. Therefore, it is important to ensure that the second and third internal supports are properly set up before the next step. At the same time, it is important to monitor the force of the support to strengthen the safety of the excavation of the DE.

Figure 14. Column diagram of axial force of interior support when load position of earthmoving vehicle is different: (**a**) first support; (**b**) second support; (**c**) third support.

Figure 15 shows the curves describing the relation between the axial force in the internal support and the load position of the earthmoving vehicle. Obviously, the value of the internal support varies with the change in the load position of the earthmoving vehicle. There is a quadratic polynomial relationship between the axial force F_N and load position D of the earthmoving vehicle. Among them, the influences between the F_N of the first internal support and the load position of the earthmoving vehicle are shown in Formula (7). The second change relation is presented in Formula (8). Moreover, the third relationship is
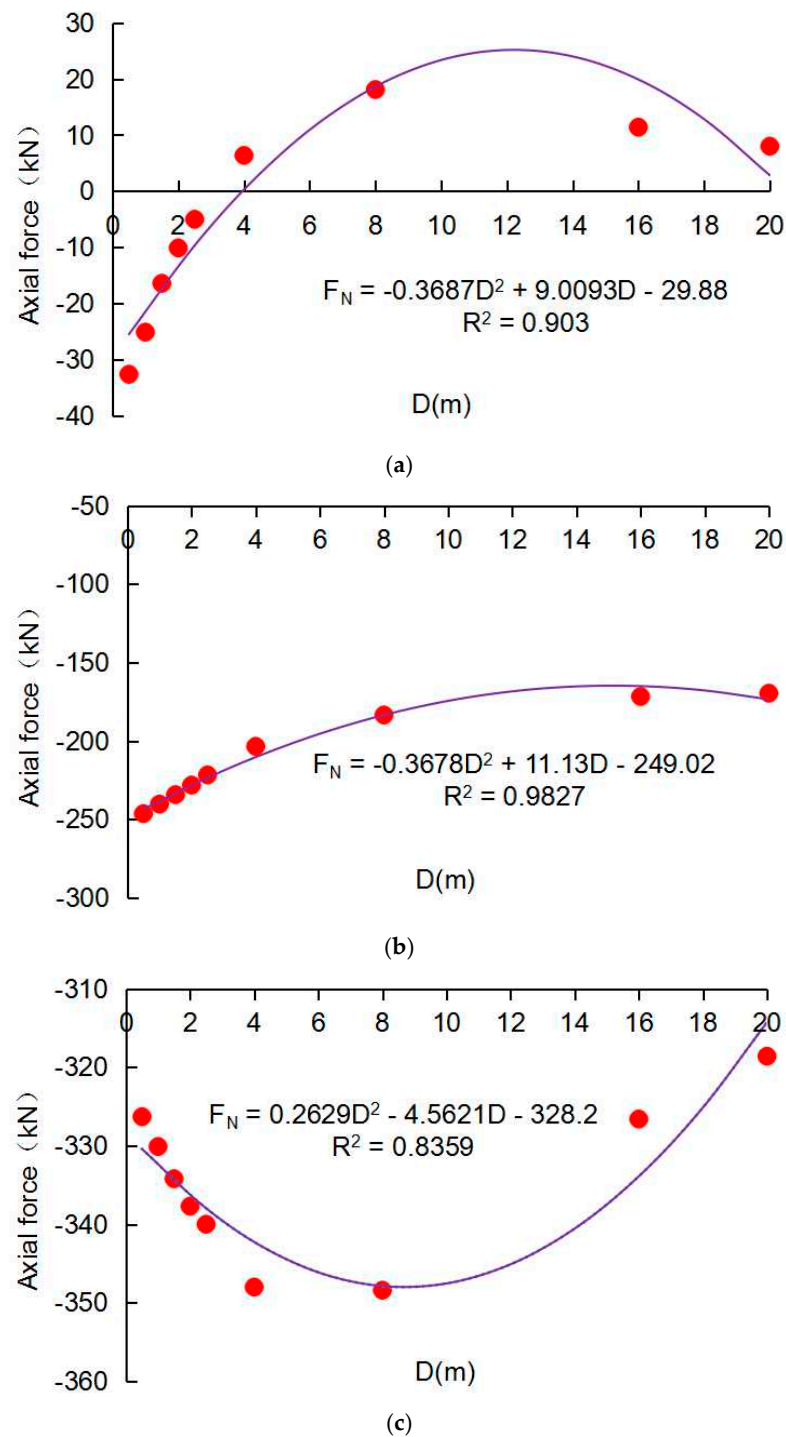
shown in Formula (9). The R^2 of F_N and D are 0.903, 0.9827, and 0.8359, respectively. In addition, the R^2 is approximately 1. This means the propinquity effect is reasonable.

$$F_N = -0.3687 D^2 + 9.0093 D - 29.88, \tag{7}$$

$$F_N = -0.3678 D^2 + 11.13 D - 249.02, \tag{8}$$

$$F_N = 0.2629 D^2 - 4.5621 D - 328.2 \tag{9}$$

(a)

(b)

(c)

Figure 15. The fitting curve of the relation between the axial force of the support and the load position of the earthmoving vehicle: (**a**) first support; (**b**) second support; (**c**) third support.

7. Discussion

According to relevant research results [39,67–69], we can find that in the past, few scholars considered the impact of the earthmoving vehicle load on the DE. In addition, the design specifications of DE, whether the impact of vehicle load near the DE needs to be considered in the design, are unclear. The method of considering this dynamic load is also not clearly stated. As a result, the discussion of the vehicle load in DE support design is relatively scarce. However, the DE will produce a large amount of earth and rocks. If it is not removed in time, it may have a certain adverse influence on the safety of the DE. In addition, earthmoving vehicles are often driven on the service road closer to the DE. An earthmoving vehicle has the features of heavy load and mobility. It perhaps has some positive influences on the stability of the DE. Therefore, the research on the safety critical value of the horizontal distance between the earthmoving vehicle and the DE has a certain theoretical and practical significance.

In view of this, this paper considers that the load distribution of earthmoving vehicles has similar characteristics to a uniform distribution. We cannot simply regard the load of earthmoving vehicles as a concentrated load. At the same time, the load characteristics of earthmoving vehicles are analyzed. In addition, we also carry out the load equivalent calculation of earthmoving vehicles. In this study, we believe that the pressure produced by the rear axle of the earthmoving vehicle is the main load of the earthmoving vehicle. The force acting on the road by the rear axle of the earthmoving truck is simplified as the uniform load. The actual most unfavorable load condition of site construction is taken into account. The results of the simulation are close to those of monitoring. It is proved that the load equivalence of this study is feasible and the choice of structure is feasible. It also reflects the rationality of the DE. In addition, it also reveals the equivalent conditions of the earthmoving vehicle load in this research are relatively reliable. In addition, this study found that the safety critical value of the horizontal distance between the earthmoving vehicle and the DE is 1 m under the given conditions in this study. When D is less than the safety critical value, the DE is in an unsafe state. This requires significant attention from the site construction personnel. The site staff should strengthen the management of earthmoving vehicles on the construction site and conduct orderly guidance. At the same time, they need to ensure that the distance between the edge of the route for the earthmoving vehicle and the DE is even bigger than 1 m. Furthermore, we can find that the deformation characteristics and mechanical performance of the DE structures under the load of an earthmoving vehicles are obviously different from those under normal symmetrical conditions and small loads. Therefore, we should pay attention to the adverse effects of the change in the load position of earthmoving vehicles on DE.

It should be noted that there are many major participants in the foundation pit excavation project. For example, the investor, the designer, and the constructor. In the design stage, if the design unit does not take into account the impact of the earthmoving truck load on the foundation pit that may appear in the actual project, safety can be compromised. Then, when the load of a fully loaded earthmoving truck acts on the foundation pit at a close distance, it may cause damage to the supporting structure of the foundation pit, a continuous collapse of the foundation pit and even loss of life and property. Therefore, the design unit needs to comprehensively consider the actual environment of the foundation pit during the design stage. In addition, if the design unit considers the actual situation and the load of the earthmoving vehicle, designs the supporting structure of the foundation pit and puts forward some requirements, safety can be ensured However, in the construction stage, the relevant management personnel of the construction unit did not carry out effective management according to the guidance of the design, resulting in the load of the earthmoving vehicle being too close to the foundation pit or the vehicle being too heavy. It may also cause the destruction of the supporting structure and even cause the continuous collapse of the foundation pit. It could also result in loss of life and property. Therefore, both the design side and the construction side can obtain some insight and knowledge from this study.

In addition, through this study, we find that the load of earthmoving vehicles will pose a threat to the stability and safety of DE. Therefore, in the design stage, the designer should take the adverse load of earthmoving vehicles that may appear in the excavation stage as one of the influencing factors for comprehensive consideration. The critical value between the load of the earthmoving vehicle and the distance of DE is obtained through analysis and calculation. Then, a more reliable supporting structure and reasonable construction arrangement are chosen. In addition, during the construction phase, the management personnel of the construction site need to manage the excavation of the DE at the construction site. There is also a need to manage the transport of earthmoving vehicles. On one hand, it is necessary to control the load of earthmoving vehicles; on the other hand, it is necessary to control the distance between the edge of the road and the DE of the earthmoving vehicles to be less than the critical value. This is conducive to ensuring the smooth progress of the DE.

However, the DE is regional. The environment in different regions is always different, for example, different geological conditions different weather and different facilities near the foundation pit. In addition, the shape, depth, size and support form of the DE are different. In addition, earthmoving vehicles have many uncertainties, such as speed changes, load changes and cyclic loading characteristics. These uncertain factors will affect the DE. The limitations of this study are as follows: only using the static method, the influence of the load position change in the earthmoving vehicle on the internal force and displacement of the excavation envelope from the horizontal distance between the earthmoving vehicle and the deep foundation pit is studied. The research content is not rich enough. The research method is relatively simple. In addition, the actual weather conditions at the construction site were not taken into account. There is room for further enrichment. The next research will further carry out other related research on the influence of the earthmoving vehicle load on DE on the basis of the accumulated experience in this study. The main research areas include the following: Firstly, the mobility characteristics of vehicles are considered and the dynamic effects of vehicle loads are incorporated into the governing equation. Secondly, the impact of the speed of the moving load on the resulting elastic field is considered. Thirdly, Biot's model is used to express the constitutive equations of various soils. Fourthly, the inclusion parameter study is conducted to determine the effect of the influencing factors on the main mechanical response of the structure. Last but not least, the influence of rainfall and excavator on the excavation of the foundation pit, and so on, is considered. The development of this research area will further enrich the results on the influence of earthmoving vehicle load conditions on DE.

8. Conclusions

In this paper, the behavior of a DE under an earthmoving vehicle load is studied. The research content mainly includes three parts. First, this paper expounds the characteristics of an earthmoving vehicle load and analyzes the equivalent treatment of the load generated by earthmoving vehicles. Secondly, a software is used to numerically simulate the excavation and support under the effect of earthmoving vehicle load. Thirdly, the deformation rule of the DE support structure under the load of earthmoving trucks is studied. Finally, on this basis, the influence of *D* on the support structure and its safety critical value is studied. The following conclusions can be drawn.

(1) On the basis of the modified Mohr–Coulomb constitutive model, MIDAS GTS NX is used to simulate the whole course of the excavation and support. The horizontal displacement and deformation of DE structures caused by excavation under the load of an earthmoving vehicle are studied. The comparison between simulation data and measured data verifies the rationality of the model.

(2) The UDW is the main component where horizontal displacement occurs. The displacement image of the structure presents asymmetrical graphic features. The reinforcement of the two sides of the enclosure structure should be considered separately according to the load of the earthmoving vehicle. As the distance *D* between the load of

the earthmoving truck and the DE decreases continuously, the displacement of the UDW becomes larger near the side of the load of the earthmoving truck and the maximum value is generated at the top of the structure. When D = 20 m, the maximum displacement is 8.2 mm. When D = 0.5 m, the maximum value is 26.8 mm. The maximum value increased by about 227%. The safety critical value of D is 1 m, and when D is less than the safety critical value, the DE is in an unsafe condition.

(3) The bending moment diagram of the UDW is in the shape of an "S". The UDW is the main bending component. The maximum value increases with the decrease in D. When D = 20 m, the maximum value is 123.9 kN·m. When D = 0.5 m, the maximum value is 193.6 kN·m. The maximum value is increased by about 56%. The position of the maximum value of the UDW varies with the variation in the load position D of the earthmoving vehicle. When D < 4 m, it appears at the junction of the second support and the UDW. When D $\geq$ 4 m, it appears at the junction of the third support and the UDW.

(4) The support axis force diagram is "rectangular". When D = 20 m, it decreases to D = 0.5 m, and the force of the first support exhibits a trend of "first increasing, then decreasing, and then increasing". When D = 20 m, the value is +8 kN, and the internal support is strained. When D = 0.5 m, the maximum value is −32.6 kN, and the internal support is compressed. The axial force of the second support shows a trend of "increasing". When D = 20 m, the axial force is −169.6 kN. When D = 0.5 m, the maximum value appears, which is −246.4 kN. The axial force value is increased by about 45%. The force of support in the third channel displayed a trend of "first increase, then decrease". When D = 20 m, the value is −318.6 kN. When D = 8 m, the maximum value is −348.4 kN. Also, the value increased by about 9.4%. When D = 0.5 m, the value is −326.3 kN. The value is reduced by about 6.3%. Both the second and third support axial forces are pressures, and the third support axial forces are the largest.

(5) For the DE under the earthmoving vehicle load, when designing and excavating the DE, the whole analysis of the DE should be carried out, and the effect of the earthmoving vehicle load on both sides of the DE should be considered comprehensively. Simultaneously, the personnel responsible for managing the construction site must strengthen their oversight and implement appropriate measures to minimize the negative impact of an earthmoving vehicle load, thereby ensuring construction safety.

References

1. Ge, X. Deformation Effects of Deep Foundation Pit Excavation on Retaining Structures and Adjacent Subway Stations. *Buildings* **2024**, *14*, 2521. [CrossRef]
2. Fu, R. A Fully Prefabricated Pile-Wall Composite Scheme of Open-Cut Tunnel and the Mechanical Behavior of the Composite Structure during Construction. *Buildings* **2024**, *14*, 1693. [CrossRef]

3.   Wu, C. Study on the Impact of Deep Foundation Pit Construction on Nearby Elevated Structures—Case Study. *Buildings* **2024**, *14*, 2541. [CrossRef]

4.   Guo, P.; Wang, Y.; Gong, X.; Lin, H.; Zhao, Y. Analysis of observed performance of a deep excavation straddled by shallowly buried pressurized pipelines and underneath traversed by planned tunnels. *Tunn. Undergr. Space Technol.* **2023**, *132*, 104946. [CrossRef]

5.   Shao, Y. Construction Mechanical Characteristics and Monitoring Analysis of the Existing Subway over the Newly Built Long Foundation Pit. *Buildings* **2024**, *14*, 2385. [CrossRef]

6.   Guo, P.; Gong, X.; Wang, Y.; Lin, H.; Zhao, Y. Minimum cover depth estimation for underwater shield tunnels. *Tunn. Undergr. Space Technol.* **2021**, *115*, 104027. [CrossRef]

7.   Guo, P.; Gong, X.; Wang, Y. Displacement and force analyses of braced structure of deep excavation considering unsymmetrical surcharge effect. *Comput. Geotech.* **2019**, *113*, 103102. [CrossRef]

8.   Gui, M.; Rajak, R.P. Responses of Structural Components of a Full-Scale Nailed Retaining Structure under the Influence of Surcharge Loading and Nail Head Configuration: A Numerical Study. *Buildings* **2023**, *13*, 561. [CrossRef]

9.   Guo, P.; Liu, F.; Lei, G.; Li, X.; Zhu, C.W.; Wang, Y.; Lu, M.; Cheng, K.; Gong, X. Predicting Response of Constructed Tunnel to Adjacent Excavation with Dewatering. *Geofluids* **2021**, *2021*, 1–17. [CrossRef]

10. Wang, Y.; Liu, J.; Guo, P.; Zhang, W.; Lin, H.; Zhao, Y.; Ou, Q. Simplified Analytical Solutions for Tunnel Settlement Induced by Axially Loading Single Pile and Pile Group. *J. Eng. Mech.* **2021**, *147*, 12. [CrossRef]

11. Guo, P.; Lei, G.; Luo, L.; Gong, X.; Wang, Y.; Li, B.; Hu, X.; Hu, H. Soil Creep Effect on Time-Dependent Deformation of Deep Braced Excavation. *Adv. Mater. Sci. Eng.* **2022**, *2022*, 5655592. [CrossRef]

12. Uge, B.U.; Guo, Y.; Zhao, J.; Liu, Y. Large-Scale 1-g Model Tests on the Interaction Between Excavation Support Structure and Nearby Multi-Type Cushioned Piled Rafts: A Comparative Study. *Iran. J. Sci. Technol. Trans. Civ. Eng.* **2024**, *48*, 1547–1571. [CrossRef]

13. He, M.; Sui, Q.; Tao, Z. Excavation compensation theory and supplementary technology system for large deformation disasters. *Deep. Undergr. Sci. Eng.* **2023**, *2*, 105–128. [CrossRef]

14. Wang, R.S.; Guo, C.C.; Lin, P.Y.; Wang, F.M. Excavation response analysis of prefabricated recyclable support structure for water-rich silt foundation pit. *Rock Soil Mech.* **2023**, *44*, 843–853. [CrossRef]

15. Haque, M.F.; Ansary, M.A. Seismic performance of concrete tunnel–sand–pile interaction by the shake table test. *Deep. Undergr. Sci. Eng.* **2024**, 1–21. [CrossRef]

16. Xia, M.; Lv, S.M.; Ren, G.M. Influence of Pile Anchor Design Parameters on Deformation of Deep Foundation Pit. *Soil Mech. Found. Eng.* **2024**, *61*, 130–137. [CrossRef]

17. Ren, D.; Kang, C.; Peng, T.; Li, Y.; Wang, J. Deformation Behavior of a Large-Scale Excavation and the Effect of an Adjacent Foundation Pit on the Excavation. *Int. J. Civ. Eng.* **2024**, *22*, 1493–1505. [CrossRef]

18. Wang, G.; Chen, W.; Cao, L.; Li, Y.; Liu, S.; Yu, J.; Wang, B. Retaining Technology for Deep Foundation Pit Excavation Adjacent to High-Speed Railways Based on Deformation Control. *Front. Earth Sci.* **2021**, *9*, 735315. [CrossRef]

19. Liu, Q. Stability Investigation of Fully Recycled Support System of Steel-Pipe-Anchored Sheet Pile in Soft Soil Excavation. *Appl. Sci.* **2024**, *14*, 5485. [CrossRef]

20. Ge, C.; Yang, M.; Li, P.; Zhang, M.; Zhang, Z. Performance and environmental impacts of deep foundation excavation in soft soils: A field and modeling-based case study in Nanjing, China. *Undergr. Space* **2024**, *18*, 218–238. [CrossRef]

21. Wang, D.Y.; Wu, K.; Wang, J.; Deng, K.F. Deformation Monitoring and Simulation Analysis of Deep Foundation Excavation Construction for subway station. *IOP Conf. Ser. Earth Environ. Sci.* **2020**, *580*, 012027. [CrossRef]

22. Zhang, Z.; You, X.; Zhang, C.; Li, W.; Zhang, M. Study on the critical stable height of vertical excavation in rocky foundation pit within layered structural plane. *Sci. Rep.* **2024**, *14*, 12191. [CrossRef]

23. Zhang, C.; Zhu, Z.; Wang, S.; Ren, X.; Shi, C. Stress wave propagation and incompatible deformation mechanisms in rock discontinuity interfaces in deep-buried tunnels. *Deep. Undergr. Sci. Eng.* **2022**, *1*, 25–39. [CrossRef]

24. Jiang, N.; Zhu, B.; He, X.; Zhou, C.; Luo, X.; Wu, T. Safety assessment of buried pressurized gas pipelines subject to blasting vibrations induced by metro foundation pit excavation. *Tunn. Undergr. Space Technol.* **2020**, *102*, 103448. [CrossRef]

25. Yu, P.; Liu, H.; Wang, Z.; Fu, J.; Zhang, H.; Wang, J.; Yang, Q. Development of urban underground space in coastal cities in China: A review. *Deep. Undergr. Sci. Eng.* **2023**, *2*, 148–172. [CrossRef]

26. Guan, L.X.; Chang-Jie, X.U.; Wang, X.P.; Xia, X.Q.; Ke, W.H. Analytical solution of deformation of underlying shield tunnel caused by foundation pit excavation and dewatering. *Rock Soil Mech.* **2023**, *44*, 3241–3251.

27. Zhu, Q.X.; Qin, H.L.; Song, B.W.; Wang, L.; Lü, X.L. A case study of the response of support structure and stratum deformation caused by deep foundation pit excavation in soft area. *IOP Conf. Ser. Earth Environ. Sci.* **2024**, *1336*, 012024. [CrossRef]

28. Liu, B.; Wu, W.; Lu, H.; Chen, S.; Zhang, D. Effect and control of foundation pit excavation on existing tunnels: A state-of-the-art review. *Tunn. Undergr. Space Technol.* **2024**, *147*, 105704. [CrossRef]

29. Li, H.; Liu, B.; Li, L.; Zhang, Q.; Huang, C. A Theoretical Solution of Deformation and Stress Calculation of the Underlying Tunnel Caused by Foundation Pit Excavation. *KSCE J. Civ. Eng.* **2024**, *28*, 2399–2408. [CrossRef]

30. Li, Z.; Zhao, G.F.; Deng, X.; Zhu, J.; Zhang, Q. Further development of distinct lattice spring model for stability and collapse analysis of deep foundation pit excavation. *Comput. Geotech.* **2022**, *144*, 104619. [CrossRef]

31. Wang, K.; Gao, Y.; Jin, Z.; Zhou, X.; Chen, L.; Zhang, C. Research on stability of steep bank slope and reserved thin-walled rock cofferdam during excavation of intake foundation pit. *Eng. Fail. Anal.* **2022**, *141*, 106659. [CrossRef]

32. Yu, C.; Long, J.; Lu, M. Study on the influence of deep foundation pit excavation on adjacent metro structure. *IOP Conf. Ser. Earth Environ. Sci.* **2021**, *768*, 012101. [CrossRef]

33. Cheng, K.; Riqing, X.; Ying, H.W.; Cungang, L.; Gan, X. Simplified method for calculating ground lateral displacement induced by foundation pit excavation. *Eng. Comput.* **2020**, *37*, 2501–2516. [CrossRef]

34. Yang, J. A discussion of the Prandlt calculation formula for anti-uplift stability of the bottom of a foundation pit wall in deep soft soil areas. *Hydrogeol. Eng. Geol.* **2021**, *48*, 61–69. [CrossRef]

35. Yin, Q.; Fu, H. Analysis of Foundation Pit Excavation Deformation and Parameter Influence of Pile-Anchor-Ribbed-Beam Support System. *Appl. Sci.* **2023**, *13*, 2379. [CrossRef]

36. Wang, H.; Zhao, Y.; Liu, J.; Ma, J. and Li, Z. Numerical Simulation of Double-row Piles in Deep Foundation Pit Excavation. *IOP Conf. Ser. Earth Environ. Sci.* **2024**, *2736*, 012005. [CrossRef]

37. Hu, J.; Li, X.; Wang, C. Displacement prediction of deep excavated expansive soil slopes with high groundwater level based on VDM-LSSVM. *Bull. Eng. Geol. Environ.* **2023**, *82*, 320. [CrossRef]

38. Zhang, C.; Zhang, W.; Ying, G.; Ying, L.; Hu, J.; Chen, W. A deep learning method for heavy vehicle load identification using structural dynamic response. *Comput. Struct.* **2024**, *297*, 107341. [CrossRef]

39. Rao, P.; Meng, J.; Cui, J.; Feng, W. Stability Analysis of Unsaturated Soil Pit Under Vehicle Load. *Geotech. Geol. Eng.* **2024**, *42*, 4987–5001. [CrossRef]

40. Han, M.; Li, Z.; Jia, J.; Bao, X.; Mei, G.; Liu, L. Force system conversion mechanisms of retaining structures for subway excavation in soft soil. *Bull. Eng. Geol. Environ.* **2023**, *82*, 262. [CrossRef]

41. Zhao, L.; Jiang, D.; Zhao, G.; Sun, J.; Yang, G. Experimental study on the dynamic characteristics of bi-block ballastless track under the combined action of vehicle load and temperature gradient. *Constr. Build. Mater.* **2024**, *438*, 137107. [CrossRef]

42. Oladejo, O.J.; Odeyale, T.O.; Ogunleye, O.J. Urban decay and traffic load on highway in Nigeria: A study of Ibadan–Oyo road. *Environ. Dev. Sustain.* **2024**, *26*, 23385–23400. [CrossRef]

43. Zhang, X.Z.; Chen, J.; Wan, L.; Luo, W.; Xu, C. Field measurement analysis of traffic load and its influence on supporting structure of adjacent foundation pit. *J. Earthq. Eng.* **2019**, *42*, 490–497. (In Chinese) [CrossRef]

44. Ding, S.L.; Qian, D.L.; Dai, Q.Q.; Bao, S. Stability analysis of deep foundation pit under vehicle load. *J. Hefei Univ. Technol. (Nat. Sci. Ed.)* **2019**, *42*, 671–676. (In Chinese) [CrossRef]

45. Wang, Y.; Sigmund, O. Multi-material topology optimization for maximizing structural stability under thermo-mechanical loading. *Comput. Methods Appl. Mech. Eng.* **2023**, *407*, 115938. [CrossRef]

46. Zhang, L.Z.; Kang, C.B.; Zhang, Z.T. Dynamic characteristics of coal gangue subgrade filler under traffic load based on the hysteretic curves. *Sci. Rep.* **2024**, *14*, 11545. [CrossRef]

47. Zhao, P.; Sun, Y.; Wang, Z.; Guo, P. Mechanical Characteristics of Deep Excavation Support Structure with Asymmetric Load on Ground Surface. *Symmetry* **2024**, *16*, 1309. [CrossRef]

48. Ermoshin, N.A.; Bukatov, D.C.; Filippov, D.A.; Tsyba, A.C.; Stroganov, A.V. Assessment of road pavement durability taking into account the variability of the traffic load parameters. *IOP Conf. Ser. Mater. Sci. Eng.* **2020**, *862*, 022023. [CrossRef]

49. Wysokowski, A. Impact of Traffic Load Randomness on Fatigue of Steel Bridges. *Balt. J. Road Bridge Eng.* **2020**, *15*, 21–44. [CrossRef]

50. Hashemi, S.K.; Valipour, H.R.; Bradford, M.A. Effect of the Traffic Load Distribution on the Progressive Collapse of a Cable-Stayed Bridge Under Blast Load. *Int. J. Steel Struct.* **2021**, *21*, 1937–1952. [CrossRef]

51. Hu, W.; Zeng, Y.; Hu, Z.T. Determination of Passive Earth Pressure on a Cantilever Retaining Wall in a Narrow Foundation Pit Based on Logarithmic Spiral Sliding Surface. *Int. J. Geomech.* **2023**, *23*, 4023126.1–4023126.9. [CrossRef]

52. Lu, D.; Liang, J.; Du, X.; Ma, C.; Gao, Z. Fractional elastoplastic constitutive model for soils based on a novel 3D fractional plastic flow rule. *Comput. Geotech.* **2019**, *105*, 277–290. [CrossRef]

53. Du, C.; Xu, Z.; Yi, F.; Gao, J.; Shi, K. Bearing capacity mechanism of soilbagged graphite tailings. *Bull. Eng. Geol. Environ.* **2024**, *83*, 24. [CrossRef]

54. Li, G.; Li, Q.; Wang, J.; Dong, J.; Sun, Q. The Deformation Characteristics of a 40-m-Deep Excavation Supported by a Suspended Diaphragm Wall in Rock and Soil Composite Ground. *KSCE J. Civ. Eng.* **2022**, *26*, 1040–1050. [CrossRef]

55. Jiang, J. Inverse Analysis of Strata in Seepage Field Based on Regularization Method and Geostatistics Theory. *Buildings* **2024**, *14*, 946. [CrossRef]

56. Liu, J.; Nie, M.; Li, C.; Yan, J. Deformation and Numerical Simulation Analysis of Deep Foundation Pit Excavation of Nanjing Yangtze River Floodplain Metro Station. *IOP Conf. Ser. Earth Environ. Sci.* **2021**, *719*, 032040. [CrossRef]

57. Hongzhi, Q.; Jiming, K.; Zhang, Y. Analysis on Dynamic Response of the Foundation Pit Supporting Structure under Vehicle Loads. *Adv. Mater. Res.* **2013**, *790*, 638–642. [CrossRef]

58. Kang, L.; Wang, Y.; Cao, J.; Bai, S. Optimization Design of Deep Foundation Pit Support Scheme under Traffic Dynamic Load. *IOP Conf. Ser. Earth Environ. Sci.* **2021**, *632*, 022006. [CrossRef]

59. Zhu, Y.P.; Lin-Ping, W.U.; Shi, D.B.; Zhao, Z.F.; Duan, X.G. Application of nonlinear soil resistance-pile lateral displacement curve based on Pasternak foundation model in foundation pit retaining piles. *Rock Soil Mech.* **2022**, *43*, 2581–2591. [CrossRef]

60. Mao, H.; Hu, Z.; Wang, W.; Liu, Z.; Yang, H.; Li, B.; Wang, Y. Two-Stage Analysis Method for the Mechanical Response of Adjacent Existing Tunnels Caused by Foundation Pit Excavation. *Buildings* **2024**, *14*, 2246. [CrossRef]

61. Yu, Z.T.; Wang, H.Y.; Wang, W.; Ling, D.S.; Zhang, X.D.; Wang, C.; Qu, Y.H. Experimental and Numerical Investigation on the Effects of Foundation Pit Excavation on Adjacent Tunnels in Soft Soil. *Math. Probl. Eng.* **2021**, *2021*, 5587857. [CrossRef]

62. Zhang, X.; Wei, G.; Lin, X.; Xia, C.; Wei, X. Transverse Force Analysis of Adjacent Shield Tunnel Caused by Foundation Pit Excavation Considering Deformation of Retaining Structures. *Symmetry* **2021**, *13*, 1478. [CrossRef]

63. Zhao, X.; Gong, X.; Guo, P. Caisson-Bored Pile Composite Anchorage Foundation for Long-Span Suspension Bridge: Feasibility Study and Parametric Analysis. *J. Bridge Eng.* **2022**, *27*, 04022117. [CrossRef]

64. Cheng, X. Characterization of Underlying Twin Shield Tunnels Due to Foundation-Excavation Unloading in Soft Soils: An Experimental and Numerical Study. *Appl. Sci.* **2021**, *11*, 10938. [CrossRef]

65. Zeng, C.F.; Sun, H.Y.; Chen, H.B.; Xue, X.L.; Liu, Y.S.; Song, W.W. *Responses of Adjacent Building Pile to Foundation Pit Dewatering/Conference on Performance-Based Design in Earthquake. Geotechnical Engineering*; Springer International Publishing: Cham, Switzerland, 2022. [CrossRef]

66. Liu, C.; Zheng, G.; Zhang, S.Y. Effect of foundation bottom heave due to excavation on supporting system in top-down method. *J. Tianjin Univ.* **2007**, *40*, 995–1001. (In Chinese) [CrossRef]

67. Rao, P.; Meng, J.; Cui, J.; Nimbalkar, S. Field Study on Rectangular Inclined Deep Foundation Excavation in Soft Soils. *Geotech. Geol. Eng.* **2024**, *42*, 2151–2168. [CrossRef]

68. Ge, C.; Yang, M.; Li, P.; Zhang, M. Influence of deep foundation pit excavation on surrounding environment: A case study in Nanjing, China. *Acta Geophys.* **2024**, 1–22. [CrossRef]

69. Wang, H.; He, S. Monitoring and Simulation Analysis of Deep Foundation Pit Excavation of Subway Station in Watery and Weak Stratum. *Indian Geotech. J.* **2024**, 1–19. [CrossRef]